

https://dspace.org/

Zircon trace element fingerprint of changing tectonic regimes in Permian rhyolites from the Central European Lowlands

E Slodczyk; A Pietranik; A Repstock; Sarah Glynn; et al

SPRINGER
https://hdl.handle.net/10539/41663
WOS

Downloaded from a DSpace repository. https://dspace.org/

International Journal of Earth Sciences (2024) 113:779–795
https://doi.org/10.1007/s00531-024-02419-5

REVIEW ARTICLE

Zircon trace element fingerprint of changing tectonic regimes in Permian rhyolites from the Central European Lowlands

Elżbieta Słodczyk[1] · Anna Pietranik[1] · Alexander Repstock[2] · Arkadiusz Przybyło[1] · Sarah Glynn[3,4] · Réka Lukács[5,6]

Received: 16 January 2024 / Accepted: 14 April 2024 / Published online: 8 May 2024
© The Author(s) 2024, corrected publication 2024

Abstract

The late Carboniferous/early Permian post-collisional rhyolites (305–285 Ma) that formed in Central Europe have generally similar whole rock compositions to that of older Late-Variscan rhyolites (330–310 Ma). However, data compilation combining zircon age with the chemical composition of rhyolites from 20 units shows a trend of increasing zircon saturation temperature with decreasing age. This trend is particularly well identified in rhyolites from the Central European Lowlands (CEL)—consisting of the NE German and NW Polish Basin—and also correlates their location with the zircon saturation temperature increasing from SE to NW from 750°C to 850°C. We infer that these higher temperatures of zircon saturation reflect a contemporaneous change in the tectonic setting from collisional to divergent, reflecting the onset of the Central European continental rifting. This interpretation is further corroborated by the trace element compositions of the CEL zircons, which resembles zircon crystallized in a divergent setting. Interestingly, the zircon formed globally in this type of setting is chemically diverse, especially considering uranium concentration. For example, zircon from locations dominated by mafic magma fractionation, such as rhyolites from Iceland, have low U concentrations and low U/Yb ratios. On the other hand, zircon formed in rhyolites in rifted margins, like western North America, tends to have much higher U and U/Yb ratios. Such high concentrations are not observed in zircon from the CEL, suggesting that the mantle input could be higher and residence times within continental crust shorter than those for rhyolites from the Cenozoic western USA. This may, in turn, suggest that the region might have been affected by a hot spot, similar to that responsible for rhyolite formation of the Snake River Plain.

Keywords Central European Basin system · Rift-related silicic volcanism · Tectonic setting · Superheated magma · Zircon saturation

Introduction

The post-collisional late Paleozoic Central European magmatic activity ejected vast quantities of volcanic material, leading to catastrophic caldera-forming silicic supereruptions (VEI > 7, e.g., Teplice caldera, Casas-García et al. 2019; Wurzen caldera, Repstock et al. 2018), and the formation of mafic (Skaggerag-Centred Large Igneous Province, Torsvik et al. 2008) and silicic large igneous provinces (LIP) (felsic large igneous province of the NE German Basin (NE GB) and NW Polish Basin (NW PB); Paulick and Breitkreuz 2005). Continental LIPs are important sites of magma formation, as they eject large quantities of bimodal volcanic products with the predominance of rhyolites and dacites (ca. 80% of volcanic products, Bryan 2007). Although the tectonic setting of silicic LIPs is still debated (e.g., Permian to Triassic Choiyoi Magmatic Province of Chile and Argentina, Bastías-Mercado et al. 2020), they are known to be typically

✉ Elżbieta Słodczyk
elzbieta.slodczyk@uwr.edu.pl

1 Institute of Geological Sciences, University of Wrocław, Pl. M. Borna 9, 50-204 Wrocław, Poland

2 Geological Survey and Geophysics, Saxon State Office for Environment, Agriculture and Geology, Pillnitzer Platz 3, D-01326 Dresden, Germany

3 School of Geosciences, University of the Witwatersrand, Private Bag 3, Wits 2050, South Africa

4 GFZ German Research Centre for Geosciences, 14473 TelegrafenbergPotsdam, Germany

5 Institute for Geological and Geochemical Research, HUN-REN Research Centre for Astronomy and Earth Sciences, MTA Centre of Excellence, Budaörsi út 45, Budapest H-1112, Hungary

6 HUN-REN-ELTE Volcanology Research Group, ELKH, Pázmány P. Sétány 1/C, 1117 Budapest, Hungary

formed in failed continental rifts (e.g., Mesozoic Chon Aike province of Patagonia and related rocks in West Antarctica, Pankhurst et al. 1998), in linear volcanic–plutonic belts at rifted continental margins (e.g., Archean high-silica rhyolites of the Gavião Block, Brazil, Zincone et al. 2016), and—very exceptionally—complex hot spot-related systems (e.g., Snake River Plain rhyolites of southern Idaho and northern Nevada, Branney et al. 2008).

Each of these tectonic settings comprises diverse conditions, differentiation processes, and sources involved in rhyolite petrogenesis that can be tracked by analysis of major and accessory minerals. However, rhyolites are prone to post-magmatic alterations, and this record is often obliterated by low-temperature processes. However, one of the accessory minerals that survives most alterations is zircon, and it offers a fingerprint of magmatic processes. As such, it is important to consider the timing of zircon crystallization within the system, which strongly depends on the bulk rock Zr concentration and consequent zircon saturation temperature in the system. In this study, we review and summarize trace element information derived from zircon grains obtained from Permo-Carboniferous high-silica volcanic rocks drilled across the CEL encompassing the NE GB and NW PB (published by Słodczyk et al. 2023) and present the results in the tectonic context, i.e., we show that a comparison of zircon composition with a wider database may provide information on the tectonic regimes in which the studied rhyolites were generated.

Geological setting

During the late Carboniferous and Permian in Central Europe, large and voluminous volcanic centres were formed due to widespread extensional tectonics in the aftermath of the Variscan orogeny (Central European Extensional Province, Kroner and Romer 2013). Here, the volcanic edifices show remarkable similarities with the volcanic products of the Cenozoic western USA, ranging from large caldera systems formed during supereruption events (e.g., the *Bishop tuff-type* Teplice rhyolite, Breiter et al. 2001; the *monotonous intermediates* and *rhyolites* of northern Saxony, Repstock et al. 2018; Hübner et al. 2021), the eruption of a superheated rhyolitic pyroclastic flow sheet (*Snake River-type* Planitz ignimbrite, Repstock et al. 2019) to the ejection of large quantities of felsic lavas (silicic LIP of the NE GB and NE PB, Paulick and Breitkreuz 2005). By contrast with the Cenozoic USA, where extensional tectonics and the subsequent magmatic activity were caused by slab rollback and/or break-off at an active continental margin (e.g., Dickinson 2002; Best et al. 2016), the late Paleozoic magmatic activity in Central Europe is associated with a continental rift (Obst 2000; Torsvik et al. 2008; Repstock et al. 2019, 2022; Mazur et al. 2021).

The CEL consists of several smaller volcanic units situated across two countries, thus called the NE German Basin (NE GB) and the NW Polish Basin (NW PB), respectively (Fig. 1). The basin development started in the late Carboniferous in the framework of dextral transtension (Breitkreuz and Kennedy 1999), which resulted from westward movements of Gondwana relative to Laurussia (Arthaud and Matte 1977). Magmatic flare-ups occurred during the initial phase of the basin development leading to the formation of a large intracontinental volcanic zone consisting of ~ 37 000 km^3 of silica-rich calc-alkaline lavas and ignimbrites with a thickness of more than 2000 m (Benek et al. 1996; Geißler et al. 2008). In Table 1, we characterize five subprovinces distinguished within the NE GB and the NW PB. The NE GB is divided into i) Mecklenburg–Vorpommern, ii) East Brandenburg, and iii) Flechtingen–Altmark subprovinces, and the NW PB is divided into iv) Western Pomerania subbasin, and v) the Fore-Sudetic Monocline (Table 1, Fig. 1). In this study, we looked at available zircon trace element records in the volcanic successions coming from Penkun (Mecklenburg–Vorpommern), Salzwedel (from Flechtingen–Almark), Wysoka Kamieńska, (from Western Pomerania) as well as from Fehmarn (W part of the NE GB, not associated with the subprovinces; data from Słodczyk et al. 2023).

Dataset reduction

Two compiled datasets were used in this study, consisting of (1) high-silica whole rock analyses and (2) rhyolitic zircon trace element compositions; which we selected from individual localities to better control the data. In the first step, we used published whole rock data of the high-silica volcanics (mainly rhyolite with associated minor trachydacite) across Central Europe (Arikas 1986; Breiter 1995, 1997; Breiter et al. 2001; Awdankiewicz 1999; Romer et al. 2001; Casas-García et al. 2019; Repstock et al. 2018, 2019, 2022; Breitkreuz et al. 2021; Hübner et al. 2021), as we were interested in comparing them with the CEL rhyolites and subordinate trachydacites (Benek et al. 1996; Protas et al. 1995; Paulick and Breitkreuz 2005; Słodczyk et al. 2015; Żelaźniewicz et al. 2016). The prerequisite for choosing any location was the presence of data necessary to calculate zircon saturation temperature (Fig. 2). Additionally, for the sake of a more global comparison, we included data from the continental divergent zones represented by rift rhyolites of the Basin and Range Province (Hildreth and Wilson 2007 for the Bishop Tuff; Spell et al. 1990; Rowe et al. 2007 and Eichler and Spell 2020 for Jemez Mt; Foley et al. 2020 for the Peach Spring Tuff), the convergent zone represented by

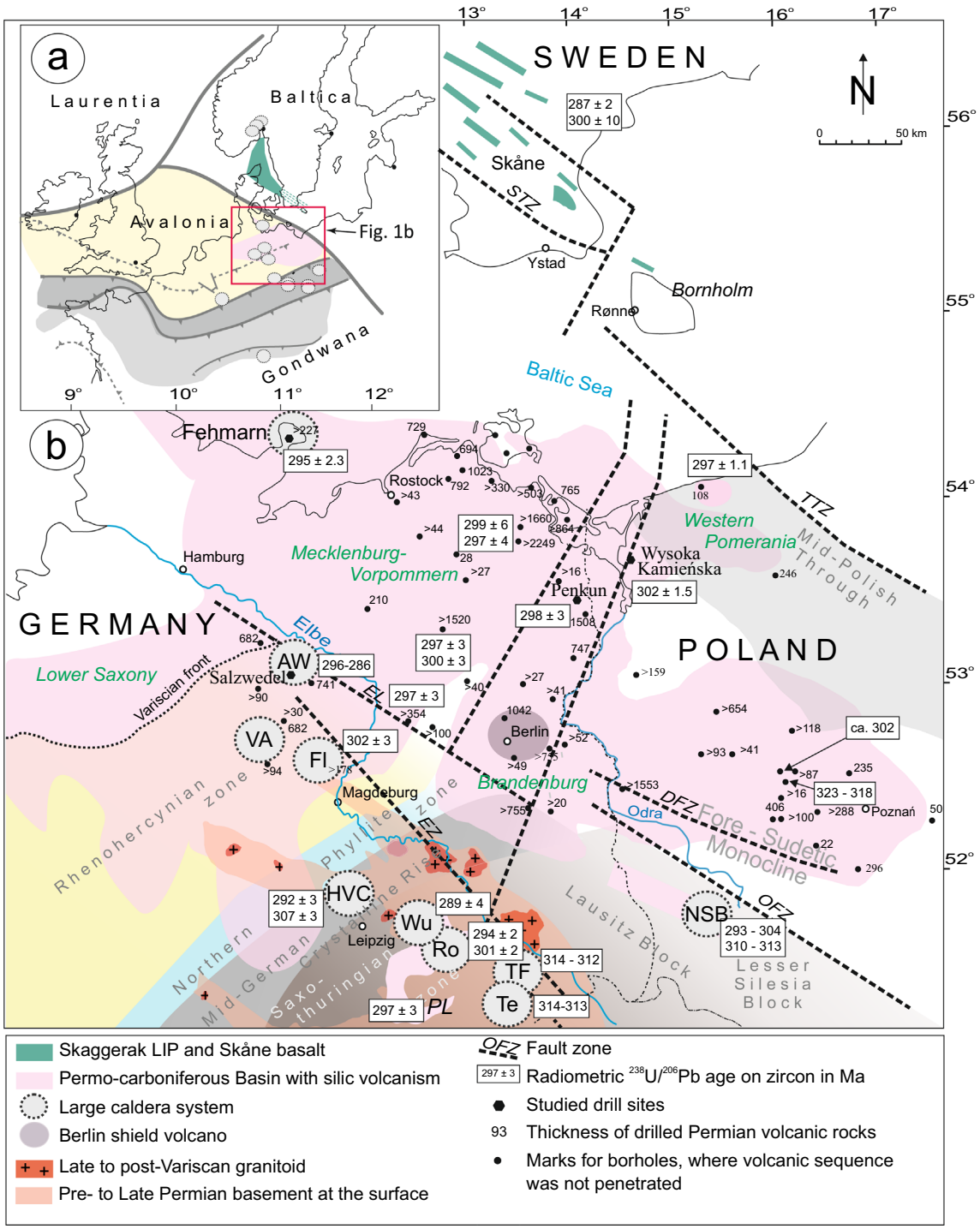


Fig. 1 Spatial distribution of Permo-Carboniferous volcanics in the Central European Lowlands with drilled depths in the NE German and the NW Polish Basin. Map modified after compilation from Benek et al. 1996; Obst 2000; Dadlez 2006; Breitkreuz et al. 2007; Geißler et al. 2008; and Torsvik et al. 2008. Radiometric $^{238}U/^{206}Pb$ ages for the zircon are taken from Breitkreuz and Kennedy 1999; Hoffmann et al. 2013; Awdankiewicz et al. 2014, Awdankiewicz 2022; Słodczyk et al. 2018; Casas-García et al. 2019; Breitkreuz et al. 2021; Tichomirowa et al. 2022 and Löcse et al. 2023. Abbreviations: volcanic systems: AW = Altmark–Wendland caldera, Fl = Flechtingen caldera, Fehmarn—assumed caldera, HVC = Halle Volcanic Complex, NSB = North Sudetic Basin rhyolites, PL = vitrophyric Planitz ignimbrite, Ro = Rochlitz caldera, Te = Teplice caldera, TF = Tharandt Forest caldera, VA = Velpke–Asse caldera, and Wu = Wurzen caldera; fault systems: DFZ = Dolsk Fault Zone, EL = Elbe Lineament, EZ = Elbe Zone, OFZ = Odra Fault Zone, STZ = Sorgenfrei Tornquist Zone TTZ = Teisseyre–Tornquist Zone

Table 1 Characteristic features of Permo-Carboniferous magmatic regions within the Central European Lowlands

Region	Characteristics
Mecklenburg–Vorpommern [Germany]	• Silica-rich successions of up to 2,300 m (base not drilled) of lava domes and flows with core and carapace faces and subvolcanic intrusions [1] • Scarcity of block-and-ash flow deposits means rare failure of lava domes [1] • Reduction in thickness toward the Rügen area (≤ 416 m) [1] • Basaltic lava fields and subvolcanic complexes [1]
East Brandenburg [Germany]	• Dominated by Mg-rich andesite lavas (with a calculated volume of ca. 8,000 km^3[2]) underlain by rhyodacitic pyroclastic deposits • The volcanic sequence reaches thickness of up to 1,700 m [1] • No sedimentary intercalations and rare immature soil horizons suggest a shield volcano edifice rather than depressions filled with lava flows [1] • 200 m lithic-rich rhyodacitic ignimbrites overlain by 750 m-thick andesitic succession with pedogenic horizons toward the top, indicating declining volcanic activity during the late stage of shield volcano evolution [1] • Andesitic succession is covered by playa sediments—the contact represents 30 Ma hiatus [4] • The volcanic rocks become more silica-rich toward the north [1]
Flechtingen– Altmark [Germany]	• Natural outcrops and quarries in Flechtingen–Roßlau Block along with deep wells with 800 m exposure of SiO_2-rich bodies [1] • The early volcanic stage is recorded in silica-rich lavas, lava domes, and laccoliths [1] • The main volcanic phase was explosive and deposited partly welded dacitic to rhyolitic ignimbrites with a thickness of up to 600 m (minimum diameter of 80 km) with a trend from lithic-rich to garnet-bearing and pumice-rich deposits [1] • Lithic-rich ignimbrites contain fragments of silica-rich lava, thus ignimbrite formation was preceded by a lava dome/laccolith (?) building phase [1] • Post-ignimbritic silica rich lava domes [1] • Existence of a large caldera system (?) or large fissure eruption accommodated within a tectonically active basin [1] • Andesitic magma forms extended sills and plugs [6] • The final volcanic stage included minor rhyolitic pyroclastic activity forming tuffs [1]
Fore-Sudetic Monocline [Poland]	• Dominated by andesites, trachyandesites with minor rhyolites, dacites, trachytes, and local basalts [3, 8, 9] • Common silicic pyroclastics, but they are minor in volume compared to subvolcanic micro-diorites, -monzonites, -granites, granites, and syenites [8] • Pyroclastic rocks of intermediate composition are rare [8] • Increasing thickness of overlaid sediments from a few hundred meters to over 5300 m northward refers to the highest subsidence rate [7, 8, 9]
Western Pomerania [Poland]	• Dominated by rhyolites and dacites with subordinate trachyandesites, andesites, and trachytes [3, 8, 9] • Silicic pyroclastics are abundant but thin, and thus of small total volume [8, 9] • Subvolcanics include microdiorite, gabbro and micromonzonite [9]

[1] Geißler et al. 2008; [2] Benek et al. 1996; [3] Jackowicz 1983, 1994, 1995, 2000, 2004; [4] Katzung 1995; [6] Awdankiewicz et al. 2004; [7] Pokorski 1988; [8] Maliszewska et al. 2008; [9] Maliszewska et al. 2016

Andean-type rhyolites (Casé et al. 2008; Mamani et al. 2010; Garrison et al. 2011; Van Zalinge et al. 2016; Andersen et al. 2017; Richards et al. 2006; Lebti et al. 2006; Bahlburg et al. 2006) and superheated and rheomorphic rhyolites of the Snake River Plain system (Pritchard et al. 2013; Coble and Mahood 2012; Ellis et al. 2010; Leeman and Bonnichsen 1982; Watts et al. 2011; Fig. 2).

In the second step, we focused on comparing zircon trace element compositions. Generally, silicic rocks contain abundant zircon and this is the case for magmas generated in different tectonic settings such as (1) convergent margins related to collisional zones (Zhao et al. 2016; Zeng et al. 2020), with the classic example of Andean-type magmatic arcs (Cisneros de León et al. 2021; Hu et al. 2013), (2) divergent tectonic lineament zones, related to continental rift volcanic (e.g., Jemez Mountain volcanic Field in New Mexico, Wu et al. 2021; Quaternary rhyolite domes of the Coso Volcanic Field in California, Burgess et al. 2021), as well as (3) intraplate settings (hot spot regime) with the well-known example of hot spot silicic volcanic activity at the Snake River Plain (Colón et al. 2015; Ellis et al. 2019) in which the Yellowstone system is included (Stelten et al. 2013, 2015, 2017; Troch et al. 2018; Till et al. 2019). Zircon compositions, representing these three tectonic settings, are compiled in Fig. 3 and the choice of localities was dependent on the availability of trace element analyses for the zircon.

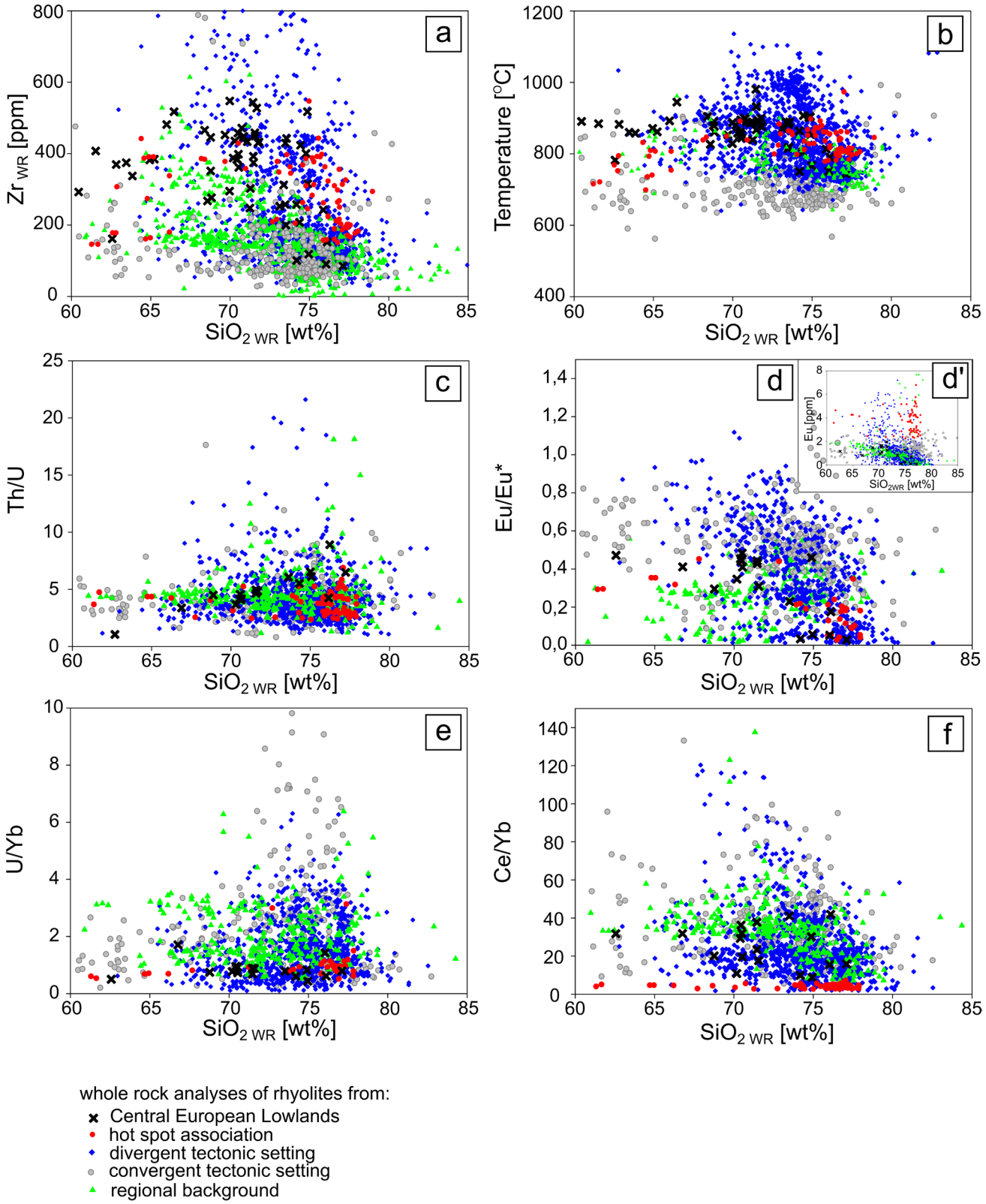
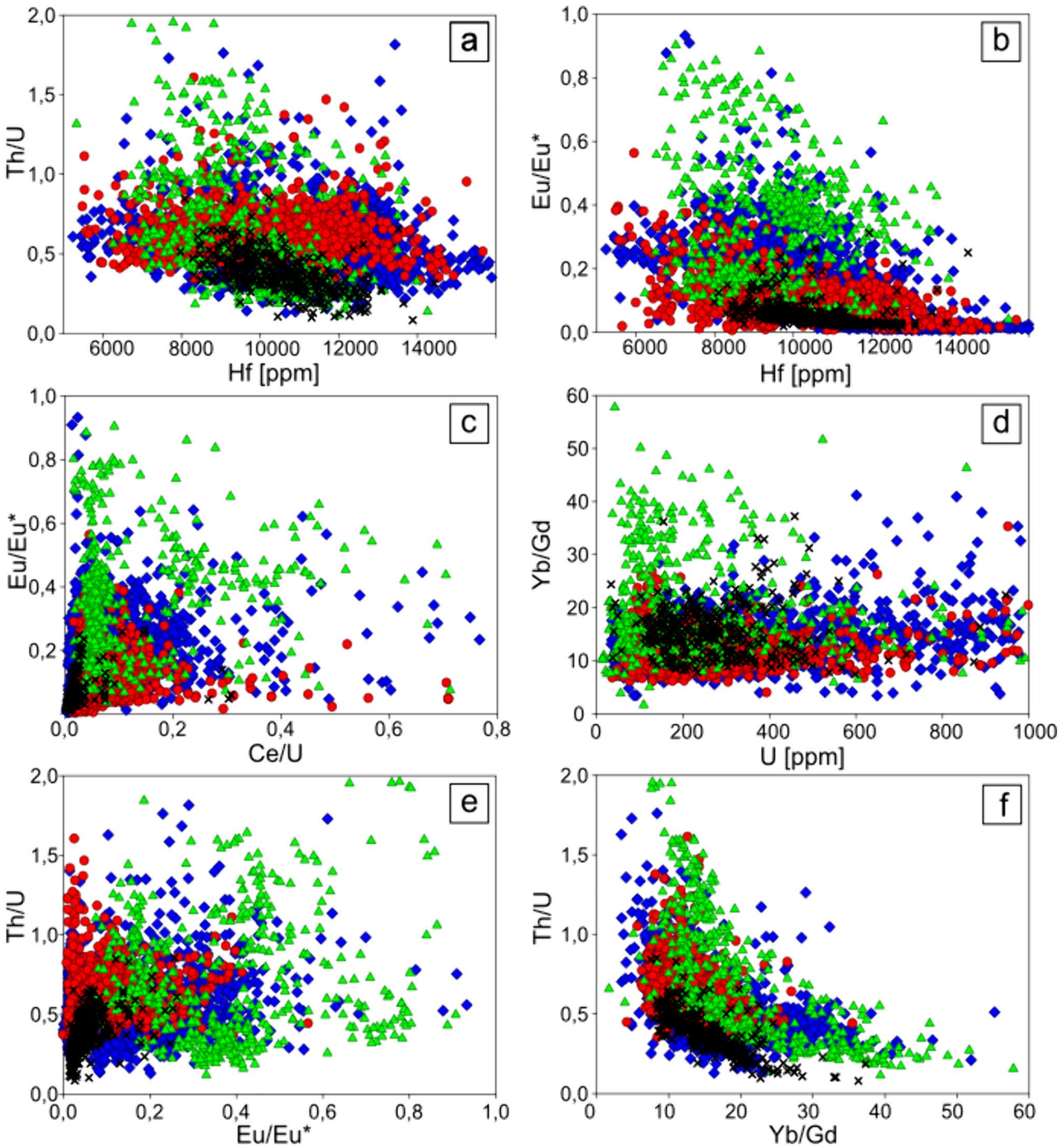


Fig. 2 Rhyolite whole rock data (**a**) SiO_2 (wt%) vs [Zr] (ppm) concentration. The CEL as indicated by the xs, are located close to the investigated sites of Fehmarn, Salzwedel, Penkun and Wysoka Kamieńska (data from: Protas et al. 1995; Benek et al. 1996; Paulick and Breitkreuz 2005; Żelaźniewicz et al. 2016); (**b**) calculated zircon saturation temperatures by formula from Boehnke et al. 2013; (**c**) Th/U vs SiO_2; (**d-d'**) Eu/Eu* and [Eu] (ppm) vs SiO_2 concentration; (**e**) U/Yb vs SiO_2; (**f**) Ce/Yb vs SiO_2


a
Th/U
Hf [ppm]
b
Eu/Eu*
Hf [ppm]
c
Eu/Eu*
Ce/U
d
Yb/Gd
U [ppm]
e
Th/U
Eu/Eu*
f
Th/U
Yb/Gd
zircon from rhyolitic rocks from given tectonic settings:
convergent type
divergent type
hot spot type
Central European Lowlands

◂**Fig. 3** Comparison of selected trace and REE compositions for zircon from rhyolites of the NE German and NW Polish Basins (data from Słodczyk et al. 2023) with zircon from rhyolites associated with variable tectonic settings. Data for divergent tectonic regimes from Burgess et al. (2021), Wall et al. (2021), Banik et al. (2018), Wu et al. (2021), Velasco-Tapia et al. (2016), Watts et al. (2016a, b), Colombini et al. (2011), Chamberlain et al. (2014). Data for zircon from rhyolites with hot spot associations from Stelten et al. (2013, 2015, 2017), Colón et al. (2015), Till et al. (2019), Ellis et al. (2019), Troch et al. (2018). Data for zircon from rhyolites from convergent regimes from Zhao et al. (2016), Hu et al. (2013) Zeng et al. (2020), Zhang et al. (2020), Cisneros de León et al. (2021), Yan et al. (2018), Wu et al. (2016)

Rhyolite magma diversity related to tectonic setting: whole rock viewpoint

Diverse trace element composition of rhyolites was linked to different tectonic settings by Bachmann and Bergantz (2008), who divided the rhyolites into two groups: (I) cold-wet oxidized rhyolites emplaced within subduction zones, and (II) hot-dry reduced rhyolites emplaced above manifestations of mantle upwelling, i.e., hot spots, ridges, and rift zones. These two groups have similar major, but variable trace element concentrations reflecting diverse fractionation paths that controlled evolution from more mafic to high-silicic magmas. In particular, the shape of the rhyolite REE patterns depend on the crystallizing mineral assemblage. The U-shape REE pattern is associated with cold-wet oxidized (I-type) rhyolites characterized by early crystallizing pyroxene, oxides, and hydrous minerals such as amphibole (Bachmann and Bergantz 2008). In contrast, the "seagull" pattern is more typical for hot-dry reduced (II-type) rhyolites dominated by fractionation of anhydrous minerals such as quartz, plagioclase, alkali feldspar, Fe–Ti oxides and clinopyroxene (based on 12 Phanerozoic compositions of rhyolites from continental mafic Large Igneous Provinces by Halder et al. 2021). These differences should be mainly reflected in the Eu anomaly with a more negative and variable Eu anomaly typical for hot-dry rhyolites that are derived from magmas that fractionated plagioclase early and a less pronounced negative Eu anomaly in cold-wet rhyolites, where plagioclase was late. However, this distinction is not well observed in our dataset in Fig. 2 with Eu anomalies characterized by similar ranges regardless of the tectonic setting and the CEL rhyolites having Eu anomaly values typical for both convergent and divergent settings. Also, LREE/HREE enrichment (Ce/Yb in Fig. 2f) seems to overlap between rhyolites and did not permit easy classification of the CEL rhyolites. From the whole rock parameters presented in Fig. 2, only Zr [ppm] shows a distinctly higher concentration in divergent settings as compared to convergent settings.

Zircon saturation and crystallization

Zirconium concentration [Zr] in magma is important because zircon stability in the magma depends on this concentration, as well as magma composition and temperature (Watson and Harrison 1983; Harrison et al. 2007; Boehnke et al. 2013). For the crystallization of zircon, the system must be saturated in zirconium [Zr], which happens at a certain temperature for a given magma composition. The chemical composition of bulk rock rhyolite can be used to calculate zircon saturation temperature (Boehnke et al. 2013). This temperature in rhyolites is often lower than the temperature recorded in major phases such as plagioclase and quartz (Pitcher et al. 2021). This difference is consistent with zircon crystallizing later than some major phases. Reconstructing the sequence of crystallization is important because it has a bearing on the interpretation of trace element concentrations in zircon, but it does not affect the temperature of zircon crystallization. This is because zircon is the main (or sole) mineral carrier of [Zr] in most evolved magmas, as the most common mineral phases incorporate very low amounts of [Zr] (< 250 ppm for clinopyroxene; < 200 ppm for amphibole; < 100 ppm for Fe–Ti oxides; < 50 ppm for biotite < 5 ppm for orthopyroxene, feldspathoids; < 1 ppm for plagioclase and alkali feldspar; 0 for quartz; Szymanowski et al. 2020). Therefore, even though zircon saturation rarely coincides with liquidus temperature, the range of zircon saturation temperatures observed for different rhyolitic units (Fig. 2b) most probably reflects differences in composition ([Zr] content) and/or temperature of magmas. The temperature and [Zr] concentration in magma might be unrelated as both mantle and crustal sources are characterized by a range of [Zr] concentrations. For example, [Zr] concentration in basalts derived from various mantle sources is between 39 and 134 ppm, with a divergent setting generally characterized by higher values (Klein 2003; data from GREM). Also, the contribution from a crustal component is of high importance, as the melting of diverse rocks may provide a variable amount of [Zr] depending on inherited zircon absence or presence within sedimentary material (e.g., Zr-poor mudstone or Zr-rich sandstone respectively; for such cases see Słodczyk et al. 2018). However, higher [Zr] concentrations of rocks with similar composition (i.e., SiO_2 content) and consequently higher zircon saturation temperatures for silicic magmas could be related to elevated temperatures of magmas (Baker et al. 2002; Boehnke et al. 2013; Watson and Harrison 1983; Zhang and Xu 2016). This is because hotter magma may dissolve inherited zircon grains in the source and incorporate Zr into the bulk rock composition (c.f. Miller et al. 2003 for hot and cold granites). Consequently, comparing zircon

saturation temperatures between different rhyolitic units having similar silica contents may be interpreted as a relative difference in the temperatures of magma from which the zircon crystallized.

Figure 2a shows that [Zr] concentrations in rhyolites from the CEL trend to higher values compared to other European rhyolites. Consequently, the CEL rhyolites are characterized by higher zircon saturation temperatures compared to the majority of Central European rhyolites with a few exceptions showing similarly high temperatures. Also, in the global context, similarly high or higher [Zr] concentrations and zircon saturation temperatures are typical for some magmas from divergent settings but are not observed in convergent settings (Fig. 2a, b). Elevated temperatures in divergent settings may represent the case where the magmatic system within a continental rift is experiencing (multiple) recharge events with a high possibility for (repeated) dissolution of incorporated zircon after each recharge (e.g., Boehnke et al. 2013; Bindeman and Melnik 2016; Zhang and Xu 2016; Cashman et al. 2017). Therefore, we suggest that a secular change in the tectonic setting in Central Europe may also be responsible for the diversity in zircon saturation temperatures between the CEL and other rhyolites. Figure 4 shows

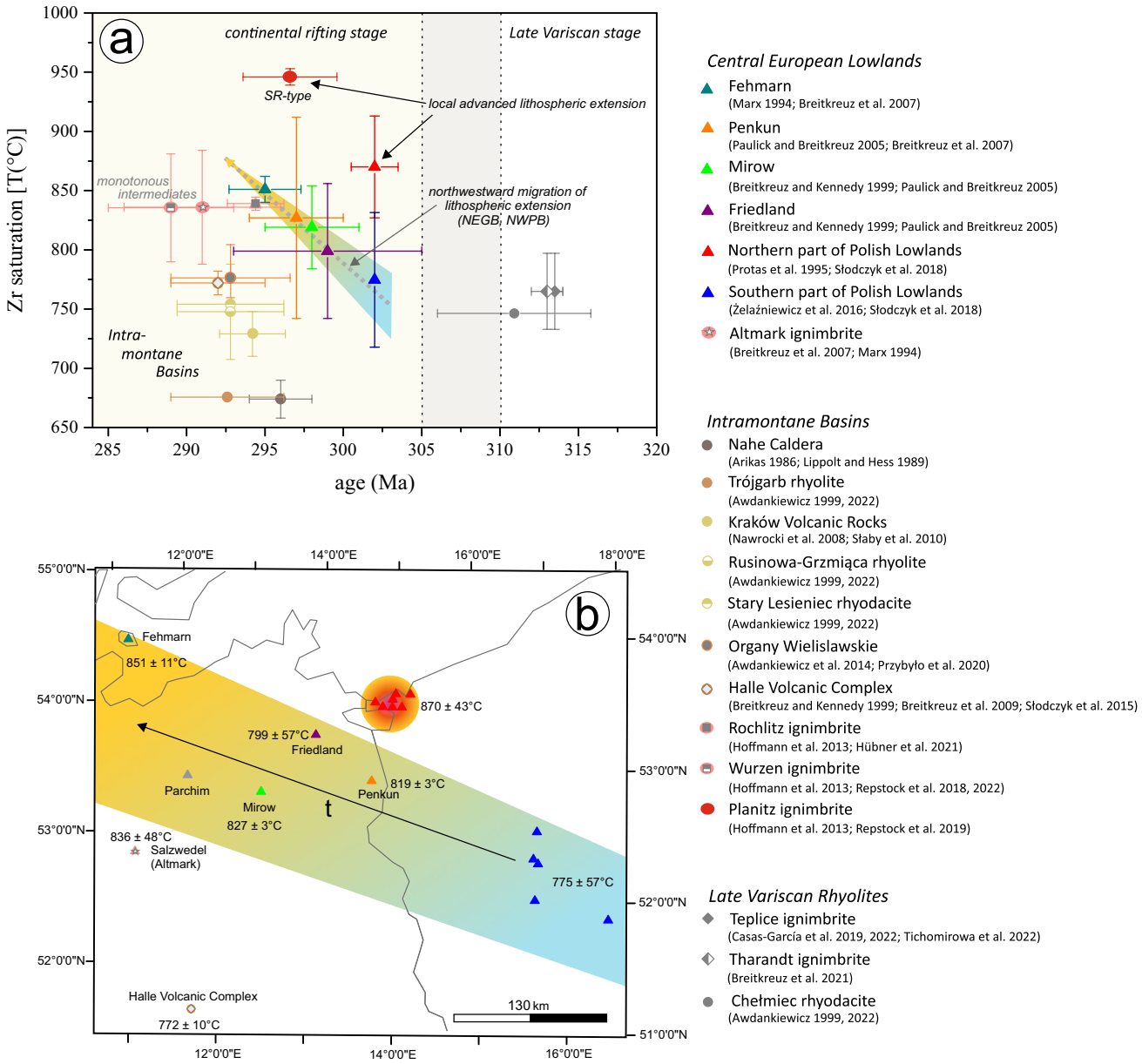


Fig. 4 (**a**) Zircon saturation temperatures of presented rhyolitic units of the Central European Lowlands with respect to their ages; (**b**) schematic illustration of alignment of regional change in zircon saturation temperature

zircon saturation temperatures plotted against the age of rhyolitic units. Older units related to the late-Variscan extension are characterized by consistent temperatures of 750–780 °C, whereas magmas younger than 305 Ma have more diverse (both lower and higher) temperatures. In the younger group a trend of increasing temperature with decreasing age can be distinguished for the CEL (Fig. 4a). This trend is correlated with the migration of the eruption centers toward the NW with time (Fig. 4b). Rhyolites recording even higher saturation temperatures occur in the Planitz ignimbrite and northern part of the NW PB, which suggests local formation of exceptionally hot magmas. Such a record of hot magmatism with some evidence of an increase in its temperature with time is consistent with mantle upwelling and lithosphere thinning that is particularly well recorded in the CEL, but some records are also preserved in intramontane basins (cf. Awdankiewicz 2022; Hübner et al. 2021; Repstock et al. 2019, 2022). Altogether the late- to post Variscan rhyolites seem to record a temporally and spatially controlled change in the tectonic setting and the predominance of hotter magmas in the Permian.

Trace elements in zircon

Observed differences in zircon saturation temperatures between Central European rhyolites and between different tectonic settings suggest that the trace elements in zircon may provide an independent record of the tectono-magmatic environment in which zircon crystallized. Such an idea was proposed by Grimes et al. 2015 (with the discrimination diagrams shown in this work) linking zircon composition to specific tectonic settings such as a mid-ocean ridge, plume-influenced ocean island, and subduction-related arc environment. In this study, we look more closely into trace element records in zircon but only from rhyolitic rocks, and our distinguished tectonic environments are therefore different

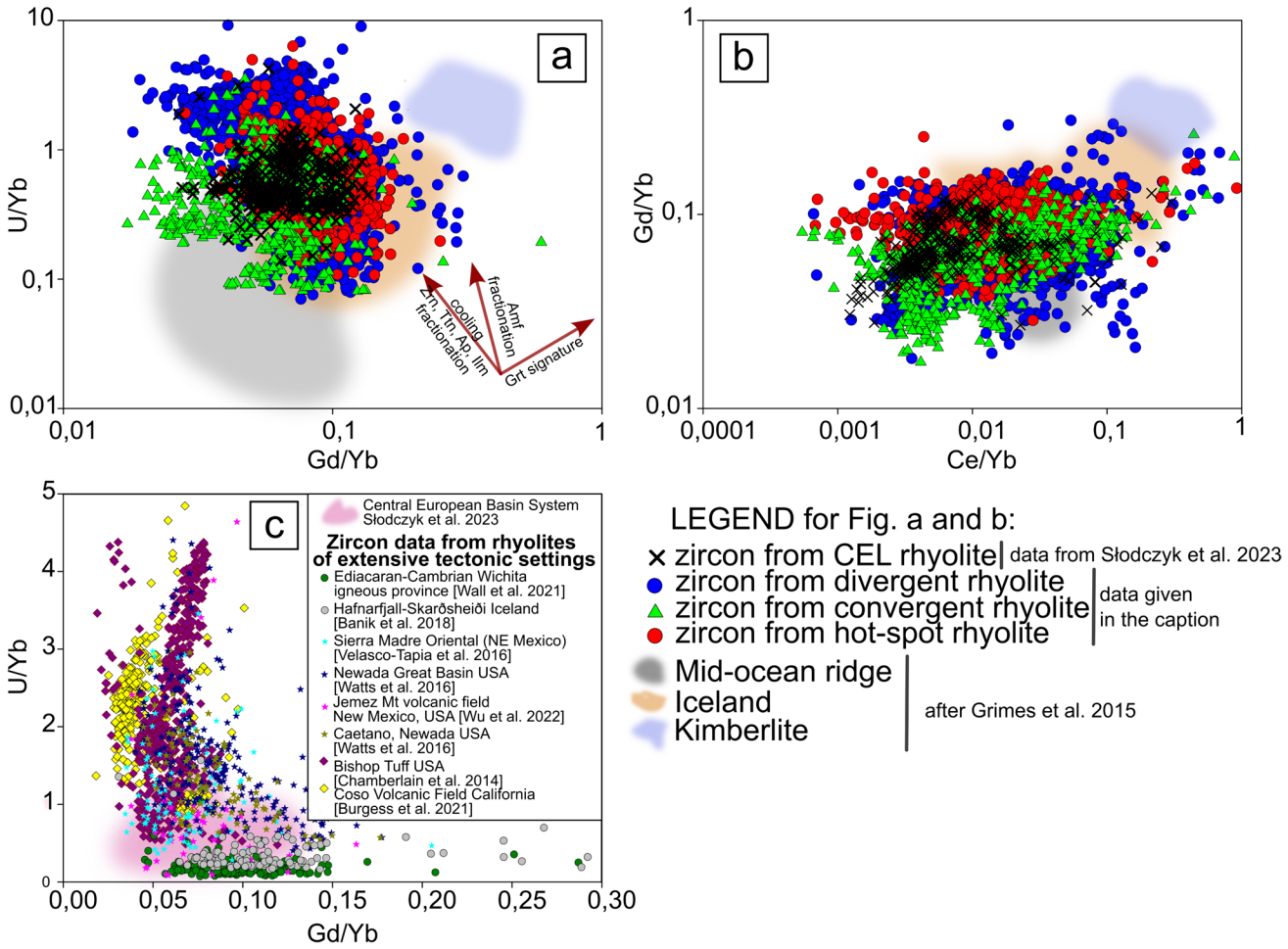


Fig. 5 (**a-b**) Zircon composition from rhyolitic units associated with variable tectonic settings (data source as in Fig. 3); determination diagram after Grimes et al. 2015; (**c**) Gd/Yb vs U/Yb ratios in zircon from rhyolitic rocks of divergent regimes (data from Wall et al. 2021; Banik et al. 2018; Velasco-Tapia et al. 2016; Watts et al. 2016a, b; Wu et al. 2021; Chamberlain et al. 2014; Burgess et al. 2021)

from those in Grimes et al. (2015). Subduction-related and hot spot settings are considered as similar locations in our and Grimes et al. (2015) datasets, but we include divergent settings that are represented by rifted margins and not by mid-ocean ridges (Fig. 5). Despite these differences, our zircon data presents a sub-set of data that plots within the compositional zircon diversity characterized by Grimes et al. (2015) (Fig. 5a and b).

The trace element composition of zircon reflects melt composition at the time of zircon saturation. This melt composition depends on the initial magma composition or the sequence of crystallization, as late crystallizing zircon composition is affected by earlier crystallizing phases. For comparison purposes, it is better to compare elemental ratios, because they are not as easily affected by local changes in melt composition. Also, ratios such as Th/U, U/Yb, Eu/Eu*, Yb/Gd, and Ce/U are linked to particular conditions, e.g., Th/U and U/Yb are thought to reflect magma evolution, Eu/Eu* and Yb/Gd show plagioclase and amphibole fractionation, respectively, and Ce/U redox conditions (Grimes et al. 2015; Kirkland et al. 2015; Burnham and Berry 2012). The magma composition may be approximated by whole rock composition and for many ratios, the rocks from all continental settings show a broadly similar range of values for some elemental ratios such as Th/U and U/Yb (Grimes et al. 2015; Fig. 2c and e, respectively). As for the Eu anomaly in whole rocks (Fig. 2d and d'), the Eu/Eu* decreases with increasing SiO_2 content, which may be interpreted as the record of plagioclase fractionation, but the decreasing trend is similar between settings. Looking at the same ratios in zircon (Fig. 3), more pronounced differences are observed for zircon than for whole rock dataset. These differences may be interpreted first in the context of crystallizing conditions specific for each tectonic setting and then applied to the CEL zircon to better identify the tectonic setting involved in their formation.

Trace elements in rhyolitic zircons from convergent tectonic settings

Generally, zircon from convergent margin rhyolites are characterized by Hf concentrations starting from ~ 7 000 to 13,500 ppm and the highest Th/U ratio up to 2 (Fig. 3a). The Th/U ratio decreases with Hf concentration. The variability of Th/U and Eu/Eu* for low Hf concentrations is the largest for this setting (Fig. 3a and b). The zircon from a convergent setting also shows higher values and variability of Yb/Gd compared to other tectonic settings (Fig. 3d and f). The high Eu/Eu* and low Yb/Gd ratios are expected of the subduction-related wet magmas that crystallize amphibole, before both plagioclase and zircon (Davidson et al. 2007), and similar trace element characteristics were noted in zircon crystallizing from wet appinitic magmas (Bruand et al. 2014; Pietranik et al. 2022). The high variability may indicate complex saturation of zircon in chemically diverse melts, where a small change in proportions of crystallizing minerals (amphibole, plagioclase, accessories) affects the evolving melt and subsequently zircon compositions (e.g., Barth et al. 2013; Grimes et al. 2015; Loader et al 2017; Lu et al. 2023).The variability may also suggest that the zircon crystallized in a compositionally stratified magma chamber (Chamberlain et al. 2014). Alternatively, for many trace element ratios the variability may indicate the incorporation of antecrystic zircons due to the reworking of a previously established crystal mush (e.g., Miller and Wooden 2004; Lukács et al. 2021). Interestingly, there is a bimodal character of zircon regarding Eu/Eu* vs Ce/U showing (a) a wide range in Eu/Eu* at low Ce/U ratios (vertical trend) and a more scattered but still visible (b) higher Ce/U ratio for variable Eu/Eu* (horizontal trend, Fig. 3c). This may reflect zircon crystallization accompanied by respective co-crystallization of plagioclase under varied redox conditions.

Altogether the trace element characteristics of zircon from a convergent margin setting are consistent with and well-illustrates crystallization of the cold-wet oxidized rhyolites recognized by Bachman and Bergantz (2008), with pyroxene, oxides, and hydrous minerals such as amphibole crystallizing before plagioclase. As such, the zircon probably records prolonged chemical evolution of magma from early (before plagioclase saturation) to late stage (when plagioclase and zircon co-crystallize). The low saturation temperatures of zircon would reflect both the cold nature of wet magmas and late zircon crystallization.

Trace elements in rhyolitic zircons from divergent and hot spot tectonic settings

Zircon from divergent settings rhyolites is characterized by a larger range of Hf concentrations, from 5 000 ppm to 16 000 ppm, than that observed in zircon from convergent settings (Fig. 3a and b). This wider range of Hf concentrations may reflect zircon crystallizing earlier in the mineral crystallization sequence or simply the hotter temperature of more dry magmas (consistent with its higher zircon saturation temperatures, Fig. 2b). On the other hand, an evolution toward higher Hf concentrations may be also due to the lack of abundant amphibole in the crystallizing sequence—a mineral that may incorporate some Hf in its structure (Nandedkar et al. 2016). Zircon from divergent setting rhyolites includes a zircon population with high U concentration accompanied by generally lower Th/U ratios (0.2–1) and extremely low Eu/Eu* values and similar zircon has been not observed in a convergent setting. This is consistent with early plagioclase fractionation (before zircon started crystallizing) and the evolution of the melt toward extremely fractionated compositions with crystallization of

an assemblage typical of dry-hot magmas, i.e., quartz, plagioclase, alkali feldspar, Fe–Ti oxides, and variable clinopyroxene (Bachmann and Bergantz 2008). However, the trace element ratios and concentrations in zircon from divergent settings change from one locality to another. Three groups can be distinguished in the diagram showing the Gd/Yb vs. U/Yb relationship (Fig. 5c) (I) increasing Gd/Yb ratio for low U/Yb typical of Iceland rhyolites (Banik et al. 2018) and early Earth crust (Ediacaran–Cambrian Wichita igneous province by Wall et al. 2021); (II) increasing U/Yb ratio for low Gd/Yb typical of the voluminous rhyolitic eruption of the Bishop Tuff in USA (e.g., Chamberlain et al. 2014); (III) mixing trend of U/Yb vs Gd/Yb typical of a mature rift system within thick continental crust represented here by rhyolitic units created within the Basin and Range Province (western USA) and also the CEL rhyolites.

Finally, the compositional diversity of the zircon from hot spot rhyolites is rather limited compared to the two previously presented tectonic settings. This is because the zircon is taken from only one locality (Yellowstone), where the general heterogeneity of potential sources is lower than in other settings. In detail, zircon from rhyolites generated within this setting have an Hf concentration ranging from 7000 to 13 000 ppm. The Th/U ratio is below 0.8 and there is no strong correlation between Th/U and Hf concentration (Fig. 3a). The Eu/Eu* anomaly for the majority of these zircon grains is below 0.2. Therefore, generally zircon from this setting is more similar to the zircon from a divergent setting, typical of dry, hot magmas.

Trace elements in zircon from NE Germany and NW Polish Basin rhyolites

Recent analyses of trace elements in zircon from the CEL were interpreted as a record of prolonged crystallization interrupted by one or two rejuvenations by more primitive magma (NE GB) or a short crystallization (NW PB, Słodczyk et al. 2023). When the zircon composition is compared to the global database, it shows rather limited variability with Th/U ratios below 0.6 (with only a few outliers up to 0.8) and Eu/Eu* below 0.1 (outliers up to 0.3). These ratios overlap with a zircon composition typical of divergent and hot spot settings, whereas zircon from a subduction-related setting has higher ratios. Therefore, all four rhyolite locations analyzed by Słodczyk et al. (2023) can be classified as hot-dry magmas characterized by early plagioclase fractionation and no amphibole crystallization. A lack of amphibole in Central European rhyolites was noted in different volcanic centers by several authors (e.g., Nahe caldera, Arikas 1986; Flechtingen caldera, Geißler et al. 2008; Altmark-Wendland caldera, Marx 1994; North Saxon Volcanic complex, Repstock et al. 2018, 2019, 2022; Hübner et al. 2021), and the zircon analyses independently confirm the dry nature of the magmas, typical of divergent settings. However, the rhyolites for this type of setting are elementally diverse between different localities (Fig. 5c), which is also well illustrated by the U concentrations in zircon (Fig. 6). The rhyolites related to divergent settings such as extensional continental margins of N America (Bishop Tuff) are commonly characterized by high U concentrations and extremely high U/Yb ratios that are observed neither in the Snake River rhyolite nor the CEL dataset (Fig. 6 a, b, c). Uranium concentration in zircon may be low for oxidized magmas, but it should be paired with high Ce/U ratios as it is the case for zircon crystallizing in a convergent setting, but not in the CEL (Fig. 3c). When the CEL zircons are compared to zircon from Bishop Tuff an evolution toward very low Eu/Eu* ratios coupled with a very high U concentration is evident only for the latter (Fig. 6b), suggesting that high U concentration marks formation of highly fractionated rhyolitic melts. Interestingly, high U concentrations are coupled with high Th/U ratios and also low Yb/Gd (Fig. 6a, c, d), which may be wrongly interpreted as crystallization from less evolved magma. The Bishop Tuff case shows that Eu/Eu* and U are better records of extreme fractionation than Th/U and Yb/Gd. Clearly, the CEL zircon does not record such fractionation, which may suggest a disruption of rhyolitic magma crystallization by the input of a more primitive magma. Therefore, even though the CEL rhyolites are said to evolve within a divergent regime during mantle upwelling, the late addition of less evolved magma portions may be interpreted as an even more intense mantle input, perhaps a sign of a hot spot fingerprint within the zircon. Such a scenario is consistent with the zircon individual grain-to-grain record (Słodczyk et al. 2023) as well as the general overlap of the CEL zircon with both divergent and hot spot zircon (Fig. 3). Input of such hot magma would prevent the extensive fractionation of rhyolitic systems that is commonly observed in rifted margins. Therefore, it seems that the CEL zircon crystallized in rhyolites that more closely resemble rhyolites from Snake River Plain rather than those from the Bishop Tuff.

Late Paleozoic rhyolites in the regional tectonic context: summary

Both zircon saturation temperatures and zircon composition in rhyolitic magmas from the CEL are consistent with an important change in the tectonic regime at the Carboniferous/Permian boundary. Zircon saturation in rhyolites can be traced from low-temperature late-Variscan to intermediate-temperature post-Variscan to high-temperature signatures. However, outstanding higher temperatures were calculated for some localities, e.g., for the Wysoka Kamieńska rhyolite, and such high temperatures are consistent with the record of trace elements in zircon from these rhyolites (Słodczyk

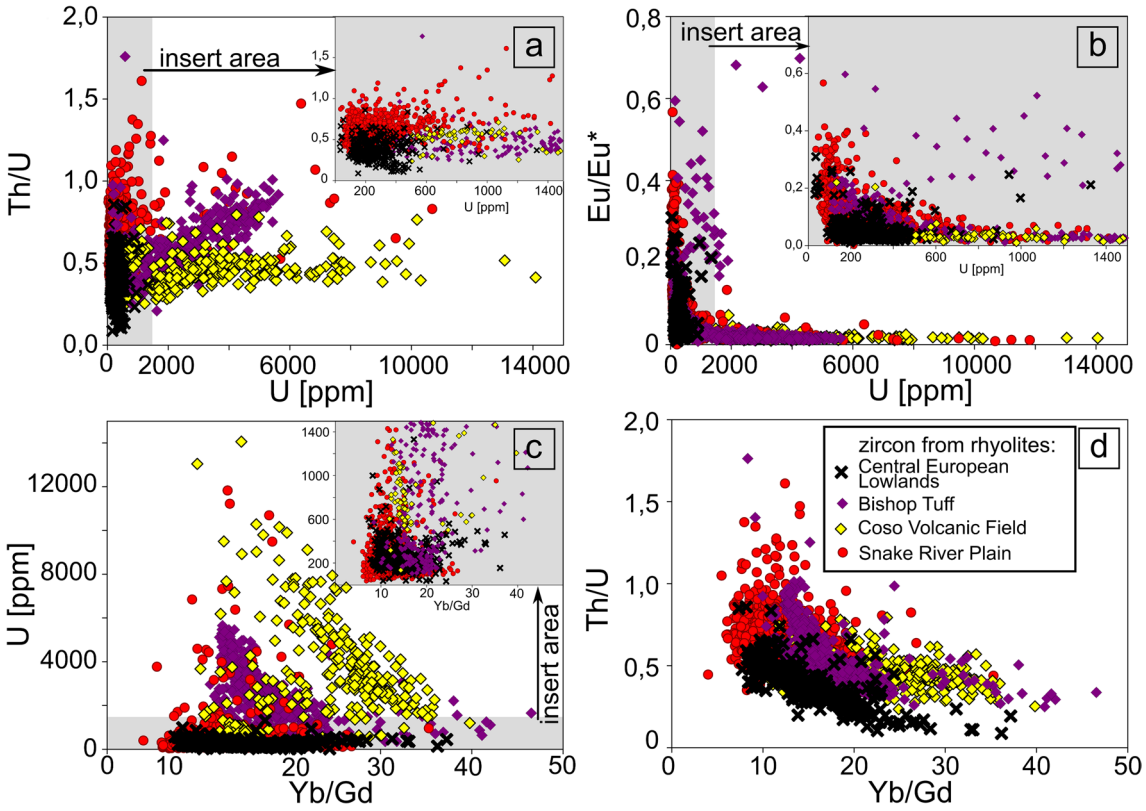


Fig. 6 Zircon composition from rhyolites of chosen tectonic settings including the CEL (NE German and NE Polish Basin data from Słodczyk et al. 2023), divergent rhyolites of the Bishop Tuff (data from Chamberlain et al. 2014), the Coso Volcanic Field (data from Burgess et al. 2021) and hot spot represented by the Snake River Plain (data as Fig. 3)

et al. 2023). This data suggests the presence of superheated mantle-derived magmas in the region.

Generally, relatively high temperatures of zircon saturation coupled with a geochemical fingerprint of crystallization in hot, dry magmas are consistent with the formation of the CEL rhyolites in divergent settings. A lack of extensive fractionation, which is typical of rhyolites formed in rifted margins (Basin and Range Province), but is absent in very primitive rifts such as Iceland may suggest that the rhyolitic magmas were affected by input from primitive magmas and evolution toward hot spot setting (such as the Snake River Plain). Similarities between the Snake River Plain volcanics in the western USA and the crystal-poor Planitz ignimbrite of the Chemnitz Basin were already observed by textural evidence, dry mineral assemblage (diopside and augite as predominant ferromagnesian phase), and thermobarometric estimations (Repstock et al. 2019). Zircon composition from the CEL is also consistent with the absence of amphibole in the crystallizing assemblage and points additionally to reduced conditions of crystallization. However, since the hot spot origin for the Snake River Plain and Yellowstone rhyolites is still debated, similarities in the trace element pattern in zircon from rhyolites of the Cenozoic Snake River Plain/ Yellowstone in the western USA and the CEL might have other complex tectonic interrelationships. Foulger et al (2015) suggest migration of lithospheric extension and subsequent crustal thinning as causes for mantle upwelling in the Snake River Plain and the adjacent Yellowstone area. Such an alternative model could also be applied to the volcanics of the CEL and its adjacent basins. The latter scenario is consistent with the spatial and temporal trend of increasing zircon saturation temperatures for progressively younger rhyolites (Fig. 4), which can be taken as evidence for crustal thinning in the Variscan foreland along the fault systems.

Perspectives

This study suggests that the CEL rhyolites formed either during migration of lithospheric extension or within the hot spot setting. The evidence in favor of migrating rift is consistent with increasing Zr saturation temperatures with age for the CEL rhyolites and successively hotter and younger rhyolite localities arranged along a regional, linear trend (Fig. 4). On the other hand, punctuated rhyolite localities recording unusually hot temperatures (Planitz in Repstock et al. 2019;

Wysoka Kamieńska in Protas et al. 1995, Słodczyk et al. 2023) accompanied by the record of short zircon crystallization (Słodczyk et al. 2023) are more consistent with hot spot influence. A better definition of the spatial arrangement of rhyolite localities with known ages, geochemistry, petrology, and in particular zircon trace element composition should better distinguish between these two scenarios. Areas recording high zircon saturation temperatures are of particular interest as they may mark important features of the basement. The occurence of such areas is consistent with the geotectonic setting of the NW European rift basins, which developed on relatively thin lithosphere (Mazur et al. 2021).

Conclusions

Increasing data on zircon trace element compositions identify this mineral as a valuable tool in recognizing tectonic setting of rhyolitic magmas formation. We showed that zircon composition differs between hot-dry (typical for rifted margins and hot spots) and cold-wet (typical for subduction settings) rhyolites and better records diverse sequences of magma evolution than whole-rock composition. We showed that the trace element composition of zircon from CEL and zircon saturation temperature are within values typical for divergent margin and hot spot dry-hot rhyolites. Zircon did not record prolonged magma evolution as observed in rhyolites from continental rifted margins (Bishop–Tuff style) and its composition indicates important input of hotter magmas before eruption. The spatial arrangement of rhyolites within the CEL suggests their evolution during migration of lithospheric extension, but occurrences of super-heated rhyolites in the area, require more data to fully constrain the setting of the rhyolite magmatism.

Acknowledgements ES, AP, and AP acknowledge financial support from the Polish National Science Centre (Narodowe Centrum Nauki) grant no. UMO-2017/25/B/ST10/00180. The authors thank Urlich Riller for editorial handling of the paper, as well as Stefan Jung for helpful comments. Constructive comments from the reviewers, Stanisław Mazur and an anonymous reviewer, helped to improve our work.

Declarations

Conflicts of interest The authors declare that they have no known competing financial interests or personal relationships that could have appeared to influence the work reported in this paper.

Open Access This article is licensed under a Creative Commons Attribution 4.0 International License, which permits use, sharing, adaptation, distribution and reproduction in any medium or format, as long as you give appropriate credit to the original author(s) and the source, provide a link to the Creative Commons licence, and indicate if changes were made. The images or other third party material in this article are included in the article's Creative Commons licence, unless indicated otherwise in a credit line to the material. If material is not included in the article's Creative Commons licence and your intended use is not permitted by statutory regulation or exceeds the permitted use, you will need to obtain permission directly from the copyright holder. To view a copy of this licence, visit http://creativecommons.org/licenses/by/4.0/.

References

Andersen NL, Singer BS, Jicha BR, Beard BL, Johnson CM, Licciardi JM (2017) Pleistocene to Holocene growth of a large upper crustal rhyolitic magma reservoir beneath the active Laguna del Maule volcanic field, central Chile. J Pet 58:85–114. https://doi.org/10.1093/petrology/egx006

Arikas K (1986) Geochemie und Petrologie der permischen Rhyolithe in Südwestdeutschland (Saar-Nahe-Pfalz-Gebiet, Odenwald, Schwarzwald) und in den Vogesen. In: 8th issue of Pollichia. Verein für Naturforschung und Landespflege Pollichia, Selbstverlag d Pollichia, p. 321.

Arthaud F, Matte P (1977) Late Paleozoic strike-slip faulting in southern Europe and northern Africa; results of a right-lateral shear zone between the Appalachians and the Urals. Geol Soc Am Bull 88:1305–1320. https://doi.org/10.1130/0016-7606(1977)88%3c1305:LPSFIS%3e2.0.CO;2

Awdankiewicz M (1999) Volcanism in a late Variscan intramontane trough: the petrology and geochemistry of the Carboniferous and Permian volcanic rocks of the Intra-Sudetic Basin, SW Poland. Geol Sudetica 32:83–111

Awdankiewicz M (2022) Polyphase Permo-Carboniferous magmatism adjacent to the Intra-Sudetic Fault: constraints from U-Pb SHRIMP zircon study of felsic subvolcanic intrusions in the Intra-Sudetic Basin, SW Poland. Int J Earth Sci 111:2199–2224. https://doi.org/10.1007/s00531-022-02232-y

Awdankiewicz M, Breitkreuz C, Ehling BC (2004) Emplacement textures in Late Palaeozoic andesite sills of the Flechtingen-Roßlau Block, north of Magdeburg (Germany). Geol Soc London Spec Pub 234:51–66. https://doi.org/10.1144/GSL.SP.2004.234.01.05

Awdankiewicz M, Kryza R, Szczepara N (2014) Timing of post-collisional volcanism in the eastern part of the Variscan Belt: constraints from SHRIMP zircon dating of Permian rhyolites in the North-Sudetic Basin (SW Poland). Geol Mag 151:611–628. https://doi.org/10.1017/S0016756813000678

Bachmann O, Bergantz GW (2008) Rhyolites and their source mushes across tectonic settings. J Pet 49:2277–2285. https://doi.org/10.1093/petrology/egn068

Bahlburg H, Carlotto V, Cárdenas J (2006) Evidence of Early to Middle Ordovician arc volcanism in the Cordillera Oriental and Altiplano of southern Peru, Ollantaytambo Formation and Umachiri beds. J South Am Earth Sci 22:52–65. https://doi.org/10.1016/j.jsames.2006.09.001

Baker DR, Conte A, Freda C, Ottolini L (2002) The effect of halogens on Zr diffusion and zircon dissolution in hydrous metaluminous granitic melts. Contrib Mineral Pet 142:666–678. https://doi.org/10.1007/s00410-001-0328-3

Banik TJ, Miller CF, Fisher CM, Coble MA, Vervoort JD (2018) Magmatic-tectonic control on the generation of silicic magmas in Iceland: Constraints from Hafnarfjall-Skarðsheiði volcano. Lithos 318:326–339. https://doi.org/10.1016/j.lithos.2018.08.022

Barth AP, Wooden JL, Jacobson CE, Economos RC (2013) Detrital zircon as a proxy for tracking the magmatic arc system: The California arc example. Geology 41:223–226. https://doi.org/10.1130/G33619.1

Bastías-Mercado F, González J, Oliveros V (2020) Volumetric and compositional estimation of the Choiyoi Magmatic Province and its comparison with other Silicic Large Igneous Provinces. J South Am Earth Sci 103:102749. https://doi.org/10.1016/j.jsames.2020.102749

Benek R, Kramer W, McCann T, Scheck M, Negendank JFW, Korich Huebscher D, Bayer U (1996) Permo-carboniferous magmatism of the Northeast German Basin. Tectonophysics 266:379–404. https://doi.org/10.1016/S0040-1951(96)00199-0

Best MG, Christiansen EH, de Silva S, Lipman PW (2016) Slab-rollback ignimbrite flare ups in the southern Great Basin and other Cenozoic American arcs: A distinct style of arc volcanism. Geosphere 12:1097–1135. https://doi.org/10.1130/GES01285.1

Bindeman IN, Melnik OE (2016) Zircon survival, rebirth and recycling during crustal melting, magma crystallization, and mixing based on numerical modelling. J Petro 57:437–460. https://doi.org/10.1093/petrology/egw013

Boehnke P, Watson EB, Trail D, Harrison TM, Schmitt AK (2013) Zircon saturation re-revisited. Chem Geol 351:324–334. https://doi.org/10.1016/j.chemgeo.2013.05.028

Branney MJ, Bonnichsen B, Andrews GDM, Ellis B, Barry TL, McCurry M (2008) 'Snake River (SR)-type'volcanism at the Yellowstone hotspot track: distinctive products from unusual, high-temperature silicic super-eruptions. Bull Volcanol 70:293–314. https://doi.org/10.1007/s00445-007-0140-7

Breiter K (1995) Geology and geochemistry of the Bohemian part of the Teplice rhyolite and adjacent post-rhyolite granites. Terra Nostra 7:20–24

Breiter K (1997) The Teplice rhyolite (Krušné hory Mts., Czech Republic) -chemical evidence of a multiply exhausted stratified magma chamber. Bull Czech Geol Surv 72:205–213

Breiter K, NovákChlupăcova JM (2001) Chemical evolution of volcanic rocks in the Altenberg – Teplice Caldera (Eastern Krûsné Hory Mts., Czech Republic, Germany). GeoLines 13:17–22

Breitkreuz C, Kennedy A (1999) Magmatic flare-up at the Carboniferous/Permian boundary in the NE German Basin revealed by SHRIMP zircon ages. Tectonophysics 302:307–326. https://doi.org/10.1016/S0040-1951(98)00293-5

Breitkreuz C, Kennedy A, Geißler M, Ehling BC, Kopp J, Muszynski A, Stouge S (2007) Far Eastern Avalonia: Its chronostratigraphic structure revealed by SHRIMP zircon ages from Upper Carboniferous to Lower Permian volcanic rocks (drill cores from Germany, Poland, and Denmark). Geol Soc Am Spec Pap 423:173–190. https://doi.org/10.1130/2007.2423(07)

Breitkreuz C, Käßner A, Tichomirowa M, Lapp M, Huang S, Stanek K (2021) The Late Carboniferous deeply eroded Tharandt Forest caldera–Niederbobritzsch granite complex: a post-Variscan long-lived magmatic system in central Europe. Int J Earth Sci 110:1265–1292. https://doi.org/10.1007/s00531-021-02015-x

Bruand E, Storey C, Fowler M (2014) Accessory mineral chemistry of high Ba–Sr granites from northern Scotland: constraints on petrogenesis and records of whole-rock signature. J Pet 55:1619–1651. https://doi.org/10.1093/petrology/egu037

Bryan S (2007) Silicic large igneous provinces. Episodes Int J Geosci 30:20–31. https://doi.org/10.18814/epiiugs/2007/v30i1/004

Burgess SD, Coble MA, Vazquez JA (2021) Zircon geochronology and geochemistry of Quaternary rhyolite domes of the Coso volcanic field, Inyo County California. J Volcanol Geotherm Res 417:107276. https://doi.org/10.1016/j.jvolgeores.2021.107276

Burnham AD, Berry AJ (2012) An experimental study of trace element partitioning between zircon and melt as a function of oxygen fugacity. Geochim Cosmochim Acta 95:196–212. https://doi.org/10.1016/j.gca.2012.07.034

Casas-García R, Rapprich V, Breitkreuz C, Svojtka M, Lapp M, Stanek K, Linnemann U (2019) Lithofacies architecture, composition, and age of the Carboniferous Teplice Rhyolite (German–Czech border): Insights into the evolution of the Altenberg-Teplice Caldera. J Volcanol Geotherm Res 386:106662. https://doi.org/10.1016/j.jvolgeores.2019.106662

Casas-García R, Rapprich V, Repstock A, Magna T, Schulz B, Kochergina YVE, Breitkreuz C (2021) Crustal vs. mantle contributions in the Erzgebirge/Krušne hory Mts. magmatism: Implications for generation of zoned, A-type silicic rocks in the late-Variscan Altenberg-Teplice Caldera, Central Europe. Lithos 404: 106429. https://doi.org/10.1016/j.lithos.2021.106429

Casé AM, López-Escobar L, Danieli JC, Schalamuk A (2008) Butalón igneous rocks, Neuquén, Argentina: Age, stratigraphic relationships and geochemical features. J South Am Earth Sci 26:188–203. https://doi.org/10.1016/j.jsames.2007.11.001

Cashman KV, Sparks RSJ, Blundy JD (2017) Vertically extensive and unstable magmatic systems: a unified view of igneous processes. Science 355:3055. https://doi.org/10.1126/science.aag3055

Chamberlain KJ, Wilson CJ, Wooden JL, Charlier BLA, Ireland TR (2014) New perspectives on the Bishop Tuff from zircon textures, ages and trace elements. J Pet 55:395–426. https://doi.org/10.1093/petrology/egt072

Cisneros de León A, Schmitt AK, Kutterolf S, Schindlbeck-Belo JC, Hernández W, Sims KWW, Garrison J, Kant LB, Weber B, Wang K-L, Lee H-Y, Trumbull RB (2021) Zircon and Melt Extraction From a Long-Lived and Vertically Extensive Magma System Underneath Ilopango Caldera (El Salvador). Geochem Geophys 22:9507. https://doi.org/10.1029/2020GC009507

Coble MA, Mahood GA (2012) Initial impingement of the Yellowstone plume located by widespread silicic volcanism contemporaneous with Columbia River flood basalts. Geology 40:655–658. https://doi.org/10.1130/G32692.1

Colombini LL, Miller CF, Gualda GA, Wooden JL, Miller JS (2011) Sphene and zircon in the Highland Range volcanic sequence (Miocene, southern Nevada, USA): elemental partitioning, phase relations, and influence on evolution of silicic magma. Miner Petrol 102:29–50. https://doi.org/10.1007/s00710-011-0177-3

Colón DP, Bindeman IN, Ellis BS, Schmitt AK, Fisher CM (2015) Hydrothermal alteration and melting of the crust during the Columbia River Basalt-Snake River Plain transition and the origin of low-δ18O rhyolites of the central Snake River Plain. Lithos 224:310–323. https://doi.org/10.1016/J.LITHOS.2015.02.022

Dadlez R (2006) The Polish Basin—relationship between the crystalline, consolidated and sedimentary crust. Geol Q 50:43–58

Davidson J, Turner S, Handley H, Macpherson C, Dosseto A (2007) Amphibole "sponge" in arc crust? Geology 35:787–790. https://doi.org/10.1130/G23637A.1

Dickinson WR (2002) The Basin and Range Province as a composite extensional domain. Int Geol Rev 44:1–38. https://doi.org/10.2747/0020-6814.44.1.1

Eichler CM, Spell TL (2020) Petrogenesis of three East Fork Member rhyolites of the Jemez volcanic field, Valles caldera, New Mexico, USA. J Volcanol Geotherm Res 389:106706. https://doi.org/10.1016/j.jvolgeores.2019.106706

Ellis BS, Barry T, Branney MJ, Wolff JA, Bindeman I, Wilson R, Bonnichsen B (2010) Petrologic constraints on the development of a large-volume, high temperature, silicic magma system: The Twin Falls eruptive centre, central Snake River Plain. Lithos 120:475–489. https://doi.org/10.1016/j.lithos.2010.09.008

Ellis BS, Schmitz MD, Hill M (2019) Reconstructing a Snake River Plain 'super-eruption'via compositional fingerprinting and high-precision U/Pb zircon geochronology. Contrib Mineral Pet 174:1–16. https://doi.org/10.1007/s00410-019-1641-z

Foley ML, Miller CF, Gualda GA (2020) Architecture of a super-sized magma chamber and remobilization of its basal cumulate (Peach Spring Tuff, USA). J Pet 61:20. https://doi.org/10.1093/petrology/egaa020

Foulger GR, Christiansen RL, Anderson DL (2015) The Yellowstone "hot spot" track results from migrating basin-range extension. The Interdisciplinary Earth: A Volume in Honor of Don L. Anderson: Geol Soc Am Spec Pap 514: 215–238. doi:https://doi.org/10.1130/2015.2514(14)

Garrison JM, Davidson JP, Hall M, Mothes P (2011) Geochemistry and petrology of the most recent deposits from Cotopaxi Volcano, Northern Volcanic Zone, Ecuador. J Pet 52:1641–1678. https://doi.org/10.1093/petrology/egr023

Geißler M, Breitkreuz C, Kiersnowski H (2008) Late Paleozoic volcanism in the central part of the Southern Permian Basin (NE Germany, W Poland): facies distribution and volcano-topographic hiati. Int J Earth Sci 97:973–989. https://doi.org/10.1007/s00531-007-0288-6

Grimes CB, Wooden JL, Cheadle MJ, John BE (2015) "Fingerprinting" tectono-magmatic provenance using trace elements in igneous zircon. Contrib Mineral Pet 170:1–26. https://doi.org/10.1007/s00410-015-1199-3

Halder M, Paul D, Sensarma S (2021) Rhyolites in continental mafic large igneous provinces: petrology, geochemistry and petrogenesis. GSF 12:53–80. https://doi.org/10.1016/j.gsf.2020.06.011

Harrison TM, Watson EB, Aikman AB (2007) Temperature spectra of zircon crystallization in plutonic rocks. Geology 35:635–638. https://doi.org/10.1130/G23505A.1

Hildreth W, Wilson CJ (2007) Compositional zoning of the Bishop Tuff. J Pet 48:951–999. https://doi.org/10.1093/petrology/egm007

Hoffmann U, Breitkreuz C, Breiter K, Sergeev S, Stanek K, Tichomirowa M (2013) Carboniferous-Permian volcanic evolution in Central Europe—U/Pb ages of volcanic rocks in Saxony (Germany) and northern Bohemia (Czech Republic). Int J Earth Sci 102:73–99. https://doi.org/10.1007/s00531-012-0791-2

Hu P, Li C, Wang M, Xie C, Wu Y (2013) Cambrian volcanism in the Lhasa terrane, southern Tibet: Record of an early Paleozoic Andean-type magmatic arc along the Gondwana proto-Tethyan margin. J Asian Earth Sci 77:91–107. https://doi.org/10.1016/j.jseaes.2013.08.015

Hübner M, Breitkreuz C, Repstock A, Schulz B, Pietranik A, Lapp M, Heuer F (2021) Evolution of the Lower Permian Rochlitz volcanic system, Eastern Germany: reconstruction of an intracontinental supereruption. Int J Earth Sci 110:1995–2020. https://doi.org/10.1007/s00531-021-02053-5

Jackowicz E (1983) Ośno IG 2. Wyniki badań petrograficznych i geochemicznych. Profile Głęb Otw Wiert Inst Geol 57:60–77 ((**in Polish**))

Jackowicz E (1995) Lower Rotliegend volcanic rocks from the western part of the Polish Lowland. Terra Nostra 7:67–69

Jackowicz E (2000) Preliminary geochemical data on lateral differentiation of the Permian volcanic unit from Western Poland. Pr Spec PTM 17:175–178

Jackowicz E (1994) Permskie skały wulkaniczne północnej części monokliny przedsudeckiej. Pr. Państw. Inst. Geol. 145 (in Polish).

Jackowicz E (2004) Rozwój mineralizacji w pęcherzykach pogazowych skał wulkanicznych. W: charakterystyka wypełnień mineralnych szczelin i przestrzeni porowych na podstawie kompleksowych badań petrologicznych (E. Jackowicz i in.). Narod. Arch. Geol. PIG-PIB,Warszawa; (in Polish)

Katzung G (1995) Pra¨-Zechstein in Zentral- und Ostbrandenburg. Berl Geowiss Abh A 168:5–21 ((**in German**))

Kirkland CL, Smithies RH, Taylor RJM, Evans N, McDonald B (2015) Zircon Th/U ratios in magmatic environs. Lithos 212:397–414. https://doi.org/10.1016/j.lithos.2014.11.021

Klein EM (2003) Geochemistry of the igneous oceanic crust. Treat Geochem 3:659

Kroner U, Romer RL (2013) Two plates—many subduction zones: the Variscan orogeny reconsidered. Gondwana Res 24:298–329. https://doi.org/10.1016/B0-08-043751-6/03030-9

Lebti PP, Thouret JC, Wörner G, Fornari M (2006) Neogene and Quaternary ignimbrites in the area of Arequipa, Southern Peru: Stratigraphical and petrological correlations. J Volcanol Geotherm Res 154:251–275. https://doi.org/10.1016/j.jvolgeores.2006.02.014

Leeman WP, Bonnichsen B (1982) Rhyolites of the Snake River Plain-Yellowstone Plateau province, Idaho and Wyoming: A summary of petrogenetic models. Cenozoic Geology of Idaho. Idaho Bureau of Mines and Geology Bulletin 26:193–202

Loader MA, Wilkinson JJ, Armstrong RN (2017) The effect of titanite crystallisation on Eu and Ce anomalies in zircon and its implications for the assessment of porphyry Cu deposit fertility. EPSL 472:107–119. https://doi.org/10.1016/j.epsl.2017.05.010

Löcse F, Schneider G, Linnemann U, Rößler R (2023) Carboniferous--Permian volcanic evolution in the mid-European Variscides: U-Pb LA-ICP-MS zircon ages, geochemical and petrographical constraints from the NW Saxonian Volcanic Basin (Germany). ZDGG 174. https://doi.org/10.1127/zdgg/2023/0359

Lu TY, He ZY, Klemd R (2023) Different magma differentiation processes of post-onset collision adakitic rocks in the Gangdese Batholith: Evidence from zircon trace elements. Chem Geol 620:121345. https://doi.org/10.1016/j.chemgeo.2023.121345

Lukács R, Caricchi L, Schmitt AK, Bachmann O, Karakas O, Guillong M, Molnár K, Seghedi I, Harangi S (2021) Zircon geochronology suggests a long-living and active magmatic system beneath the Ciomadul volcanic dome field (eastern-central Europe). EPLS 565; 116965. https://doi.org/10.1016/j.epsl.2021.116965

Maliszewska A, Kuberska M, Kiersnowski H, Jackowicz E (2008) Petrologia, sedymentologia i nowa litostratygrafia utworów czerwonego spagowca. Narod. Arch. Geol. PIG-PIB, Warszawa.

Maliszewska A, Jackowicz E, Kuberska M, Kiersnowski H (2016) Skały permu dolnego (czerwonego spągowca) zachodniej Polski: monografia petrograficzna. Prace Państwowego Instytutu Geologicznego, 204.

Mamani M, Wörner G, Sempere T (2010) Geochemical variations in igneous rocks of the Central Andean orocline (13 S to 18 S): Tracing crustal thickening and magma generation through time and space. Bulletin 122:162–182. https://doi.org/10.1130/B26538.1

Marx J (1994) Die permokarbonen Magmatite Nordwestdeutschlands im Vergleich zu den magmatischen Serien angrenzender Gebiete. Unpubl. PhD thesis, University of Hanover, 204. (in German)

Mazur S, Malinowski M, Maystrenko YP, Gągała Ł (2021) Preexisting lithospheric weak zone and its impact on continental rifting – the Mid-Polish Trough, Central European Basin System. Glob Planet Change 198:103417. https://doi.org/10.1016/j.gloplacha.2021.103417

Miller JS, Wooden JL (2004) Residence, resorption and recycling of zircons in Devils Kitchen rhyolite, Coso Volcanic field, California. J Petrol 45:2155–2170. https://doi.org/10.1093/petrology/egh051

Miller CF, McDowell SM, Mapes RW (2003) Hot and cold granites? Implications of zircon saturation temperatures and preservation of inheritance. Geology 31:529–532. https://doi.org/10.1130/0091-7613(2003)031%3c0529:HACGIO%3e2.0.CO;2

Nandedkar RH, Hürlimann N, Ulmer P, Müntener O (2016) Amphibole–melt trace element partitioning of fractionating calcalkalinemagmas in the lower crust: an experimental study.

Contrib Mineral Pet 171:1–25. https://doi.org/10.1007/s00410-016-1278-0

Nawrocki J, Fanning M, Lewandowska A, Polechońska O, Werner T (2008) Palaeomagnetism and the age of the Cracow volcanic rocks (S Poland). Geophys J Int 174:475–488. https://doi.org/10.1111/j.1365-246X.2008.03804.x

Obst K (2000) Permo-Carboniferous dyke magmatism on the Danish island Bornholm. Neues Jahrbuch Geologie Paläontologie 218:243–266

Pankhurst RJ, Leat PT, Sruoga P, Rapela CW, Márquez M, Storey BC, Riley TR (1998) The Chon Aike province of Patagonia and related rocks in West Antarctica: a silicic large igneous province. J Volcanol Geotherm Res 81:113–136. https://doi.org/10.1016/S0377-0273(97)00070-X

Paulick H, Breitkreuz C (2005) The Late Paleozoic felsic lava-dominated large igneous province in northeast Germany: volcanic facies analysis based on drill cores. Int J Earth Sci 94:834–850. https://doi.org/10.1007/s00531-005-0017-y

Pietranik A, Farina F, Derkowska K, Schaltegger U, Przybyło A, Storey C, Lasalle S, Dhuime B, Pańczyk M, Zieliński G, Nowak M; Bulcewicz K; Kierczak J, Kierczak J (2022) Zircon reveals diverse trends of magma crystallization from two types of early post-collisional diorites (Variscan Orogen, NE Bohemian Massif). J Pet 63: 059. https://doi.org/10.1093/petrology/egac059

Pitcher BW, Gualda GA, Hasegawa T (2021) Repetitive duality of rhyolite compositions, timescales, and storage and extraction conditions for Pleistocene caldera-forming eruptions, Hokkaido. Jpn J Pet 62:106. https://doi.org/10.1093/petrology/egaa106

Pokorski J (1988) Rotliegendes lithostratigraphy in northwestern Poland. Bull Pol Acad Sci 36:99–108

Pritchard CJ, Larson PB, Spell TL, Tarbert KD (2013) Eruption-triggered mixing of extra-caldera basalt and rhyolite complexes along the East Gallatin-Washburn fault zone, Yellowstone National Park, WY, USA. Lithos 175:163–177. https://doi.org/10.1016/j.lithos.2013.04.022

Protas A, Biernacka J, Muszyński A, Wojewoda J, Ziółkowska-Kozdrój M (1995) Pozycja geologiczna i petrologia kompleksu wulkanogenicznego permu podłoża Pomorza Zachodniego. Program Badawczy Komitetu Badań Naukowych (in Polish).

Przybyło A, Pietranik A, Schulz B, Breitkreuz C (2020) Towards Identification of Zircon Populations in Permo-Carboniferous Rhyolites of Central Europe: insight from automated SEM-mineral liberation analyses. Minerals 10:308. https://doi.org/10.3390/min10040308

Repstock A, Breitkreuz C, Lapp M, Schulz B (2018) Voluminous and crystal-rich igneous rocks of the Permian Wurzen volcanic system, northern Saxony, Germany: physical volcanology and geochemical characterization. Int J Earth Sci 107:1485–1513. https://doi.org/10.1007/s00531-017-1554-x

Repstock A, Heuer F, Im J, Hübner M, Schulz B, Breitkreuz C, Gilbricht S, Fischer F, Lapp M (2019) A Late Paleozoic Snake River-type ignimbrite (Planitz vitrophyre) in the Chemnitz Basin, Germany: Textural and compositional evidence for complex magma evolution in an intraplate setting. J Volcanol Geotherm Res 369:35–49. https://doi.org/10.1016/j.jvolgeores.2018.11.010

Repstock A, Casas-García R, Zeug M, Breitkreuz C, Schulz B, Gevorgyan H, Heuer F, Gilbricht S, Lapp M (2022) The monotonous intermediate magma system of the Permian Wurzen caldera, Germany: Magma dynamics and petrogenetic constraints for a supereruption. J Volcanol Geotherm Res 429: 107596. https://doi.org/10.1016/j.jvolgeores.2022.107596

Richards JP, Ullrich T, Kerrich R (2006) The late Miocene-Quaternary Antofalla volcanic complex, southern Puna, NW Argentina: protracted history, diverse petrology, and economic potential. J Volcanol Geotherm Res 152:197–239. https://doi.org/10.1016/j.jvolgeores.2005.10.006

Romer RL, Förster HJ, Breitkreuz C (2001) Intracontinental extensional magmatism with a subduction fingerprint: the late Carboniferous Halle Volcanic Complex (Germany). Contrib Mineral Pet 141:201–221. https://doi.org/10.1007/s004100000231

Rowe MC, Wolff JA, Gardner JN, Ramos FC, Teasdale R, Heikoop CE (2007) Development of a continental volcanic field: petrogenesis of pre-caldera intermediate and silicic rocks and origin of the Bandelier magmas, Jemez Mountains (New Mexico, USA). J Pet 48:2063–2091. https://doi.org/10.1093/petrology/egm050

Słaby E, Breitkreuz C, Żaba J, Domańska-Siuda J, Gaidzik K, Falenty K, Falenty A (2010) Magma generation in an alternating transtensional–transpressional regime, the Kraków-Lubliniec Fault Zone, Poland. Lithos 119:251–268. https://doi.org/10.1016/j.lithos.2010.07.003

Słodczyk E, Pietranik A, Breitkreuz C, Pędziwiatr A, Bokła M, Schab K, Grodzicka M (2015) Formation of a laccolith by magma pulses: Evidence from modal and chemical composition of the 500 m long borehole section through the Permo-Carboniferous Landsberg laccolith (Halle Volcanic Complex). Geochem J 49:523–537. https://doi.org/10.2343/geochemj.2.0382

Słodczyk E, Pietranik A, Glynn S, Wiedenbeck M, Breitkreuz C, Dhuime B (2018) Contrasting sources of Late Paleozoic rhyolite magma in the Polish Lowlands: evidence from U-Pb ages and Hf and O isotope composition in zircon. Int J Earth Sci 107:2065–2081. https://doi.org/10.1007/s00531-018-1588-8

Słodczyk E, Przybyło A, Pietranik A, Lukács R (2023) Diverse magma evolution recorded in trace element composition of zircon from Permo-Carboniferous rhyolites (NE German Basin, NW Polish Basin). Int J Earth Sci 112:2205–2222. https://doi.org/10.1007/s00531-023-02342-1

Spell TL, Harrison TM, Wolff JA (1990) 40Ar/39Ar dating of the Bandelier Tuff and San Diego Canyon ignimbrites, Jemez Mountains, New Mexico: temporal constraints on magmatic evolution. J Volcanol Geotherm Res 43:175–193. https://doi.org/10.1016/0377-0273(90)90051-G

Stelten ME, Cooper KM, Vazquez JA, Reid MR, Barfod GH, Wimpenny J, Yin QZ (2013) Magma mixing and the generation of isotopically juvenile silicic magma at Yellowstone caldera inferred from coupling 238 U–230 Th ages with trace elements and Hf and O isotopes in zircon and Pb isotopes in sanidine. Contrib Mineral Pet 166:587–613. https://doi.org/10.1007/s00410-013-0893-2

Stelten ME, Cooper KM, Vazquez JA, Calvert AT, Glessner JJ (2015) Mechanisms and timescales of generating eruptible rhyolitic magmas at Yellowstone caldera from zircon and sanidine geochronology and geochemistry. J Pet 56:1607–1642. https://doi.org/10.1093/petrology/egv047

Stelten ME, Cooper KM, Wimpenny JB, Vazquez JA, Yin QZ (2017) The role of mantle-derived magmas in the isotopic evolution of Yellowstone's magmatic system. Geochem Geophys 18:1350–1365. https://doi.org/10.1002/2016GC006664

Szymanowski D, Forni F, Wolff JA, Ellis BS (2020) Modulation of zircon solubility by crystal–melt dynamics. Geology 48:798–802. https://doi.org/10.1130/G47405.1

Tichomirowa M, Käßner A, Repstock A, Weber S, Gerdes A, Whitehouse M (2022) New CA-ID-TIMS U-Pb zircon ages for the Altenberg-Teplice Volcanic Complex (ATVC) document discrete and coeval pulses of Variscan magmatic activity in the Eastern Erzgebirge (Eastern Variscan Belt). Int J Earth Sci 111:1885–1908. https://doi.org/10.1007/s00531-022-02204-2

Till CB, Vazquez JA, Stelten ME, Shamloo HI, Shaffer JS (2019) Coexisting discrete bodies of rhyolite and punctuated volcanism characterize Yellowstone's post-Lava Creek Tuff caldera evolution. Geochem Geophys 20:3861–3881. https://doi.org/10.1029/2019GC008321

Torsvik TH, Smethurst MA, Burke K, Steinberger B (2008) Long term stability in deep mantle structure: Evidence from the ~300 Ma Skagerrak-Centered Large Igneous Province (the SCLIP). EPSL 267:444–452. https://doi.org/10.1016/j.epsl.2007.12.004

Troch J, Ellis BS, Schmitt AK, Bouvier AS, Bachmann O (2018) The dark side of zircon: textural, age, oxygen isotopic and trace element evidence of fluid saturation in the subvolcanic reservoir of the Island Park-Mount Jackson Rhyolite, Yellowstone (USA). Contrib Mineral Pet 173:1–17. https://doi.org/10.1007/s00410-018-1481-2

Van Zalinge ME, Sparks RSJ, Cooper FJ, Condon DJ (2016) Early Miocene large-volume ignimbrites of the Oxaya Formation, Central Andes. J Geol Soc 173:716–733. https://doi.org/10.1144/jgs2015-123

Velasco-Tapia F, Martínez-Paco M, Iriondo A, Ocampo-Díaz YZE, Cruz-Gámez EM, Ramos-Ledezma A, Andaverde JA, Ostrooumov M, Masuch D (2016) Altered volcanic ash layers of the Late Cretaceous San Felipe Formation, Sierra Madre Oriental (Northeastern Mexico): UPb geochronology, provenance and tectonic setting. J South Am Earth Sci 70: 18–35. doi:https://doi.org/10.1016/j.jsames.2016.04.010

Wall CJ, Hanson RE, Schmitz M, Price JD, Donovan RN, Boro JR, Eschberger AM, Toews CE (2021) Integrating zircon trace-element geochemistry and high-precision U-Pb zircon geochronology to resolve the timing and petrogenesis of the late Ediacaran-Cambrian Wichita igneous province, Southern Oklahoma Aulacogen, USA. Geology 49:268–272. https://doi.org/10.1130/G48140.1

Watson EB, Harrison TM (1983) Zircon saturation revisited: temperature and composition effects in a variety of crustal magma types. EPLS 64:295–304. https://doi.org/10.1016/0012-821X(83)90211-X

Watts KE, Bindeman IN, Schmitt AK (2011) Large-volume rhyolite genesis in caldera complexes of the Snake River Plain: insights from the Kilgore Tuff of the Heise Volcanic Field, Idaho, with comparison to Yellowstone and Bruneau-Jarbidge rhyolites. J Pet 52:857–890. https://doi.org/10.1093/petrology/egr005

Watts KE, Coble MA, Vazquez JA, Henry CD, Colgan JP, John DA (2016a) a) Chemical abrasion-SIMS (CA-SIMS) U-Pb dating of zircon from the late Eocene Caetano caldera, Nevada. Chem Geol 439:139–151. https://doi.org/10.1016/j.chemgeo.2016.06.013

Watts KE, John DA, Colgan JP, Henry CD, Bindeman IN, Schmitt AK (2016b) b) Probing the volcanic–plutonic connection and the genesis of crystal-rich rhyolite in a deeply dissected supervolcano in the Nevada Great Basin: source of the Late Eocene Caetano Tuff. J Pet 57:1599–1644. https://doi.org/10.1093/petrology/egw051

Wu T, Polat A, Frei R, Fryer BJ, Yang KG, Kusky T (2016) Geochemistry, Nd, Pb and Sr isotope systematics, and U-Pb zircon ages of the Neoarchean Bad Vermilion Lake greenstone belt and spatially associated granitic rocks, western Superior Province. Canada Precambrian Res 282:21–51. https://doi.org/10.1016/j.precamres.2016.06.021

Wu J, Cronin SJ, Rowe MC, Wolff JA, Barker SJ, Fu B, Boroughs S (2021) Crustal evolution leading to successive rhyolitic supereruptions in the Jemez Mountains volcanic field, New Mexico, USA. Lithos 396:106201. https://doi.org/10.1016/j.lithos.2021.106201

Yan LL, He ZY, Beier C, Klemd R (2018) Zircon trace element constrains on the link between volcanism and plutonism in SE China. Lithos 320:28–34. https://doi.org/10.1016/j.lithos.2018.08.040

Żelaźniewicz A, Oberc-Dziedzic T, Fanning CM, Protas A, Muszyński A (2016) Late Carboniferous–early Permian events in the Trans-European Suture Zone: tectonic and acid magmatic evidence from Poland. Tectonophysics 675: 227–243. https://doi.org/10.1016/j.tecto. 2016. 02. 040

Zeng YC, Xu JF, Huang F, Li MJ, Chen Q (2020) Generation of the 105–100 Ma Dagze volcanic rocks in the north Lhasa Terrane by lower crustal melting at different temperature and depth: Implications for tectonic transition. GSA Bull 132:1257–1272. https://doi.org/10.1130/B35306.1

Zhang Y, Xu Z (2016) Zircon saturation and Zr diffusion in rhyolitic melts, and zircon growth geospeedometer. Am Min 101:1252–1267. https://doi.org/10.2138/am-2016-5462

Zhang B, Liu J, Chen W, Zhu Z, Sun C (2020) Late Eocene magmatism of the eastern Qiangtang block (eastern Tibetan Plateau) and its geodynamic implications. J Asian Earth Sci 195:104329. https://doi.org/10.1016/j.jseaes.2020.104329

Zhao L, Guo F, Fan W, Zhang Q, Wu Y, Li J, Yan W (2016) Early Cretaceous potassic volcanic rocks in the Jiangnan Orogenic Belt, East China: Crustal melting in response to subduction of the Pacific-Izanagi ridge? Chem Geol 437:30–43. https://doi.org/10.1016/j.chemgeo.2016.05.011

Zincone SA, Oliveira EP, Laurent O, Zhang H, Zhai M (2016) 3.30 Ga high-silica intraplate volcanic–plutonic system of the Gavião Block, São Francisco Craton, Brazil: Evidence of an intracontinental rift following the creation of insulating continental crust. Lithos 266:414–434. https://doi.org/10.1016/j.lithos.2016.10.011